Polyhedron 30 (2011) 53–60

Contents lists available at ScienceDirect

Polyhedron

journal homepage: www.elsevier.com/locate/poly

Intra- and intermolecular hydrogen bonds in [Ag(PPh$_3$)$_3$(HL)] complexes [H$_2$L: H$_2$*x*spa = 3(aryl)-2-sulfanylpropenoic acids; H$_2$cpa = 2-cyclopentylidene-2-sulfanyl-acetic acid]

Elena Barreiro [a], José S. Casas [a], María D. Couce [b], Agustín Sánchez [a], José Sordo [a,*], José M. Varela [a], Ezequiel M. Vázquez López [b]

[a] Departamento de Química Inorgánica, Facultade de Farmacia, Universidade de Santiago de Compostela, 15782 Santiago de Compostela, Galicia, Spain
[b] Departamento de Química Inorgánica, Facultade de Química, Universidade de Vigo, 36310 Vigo, Galicia, Spain

ARTICLE INFO

Article history:
Received 27 July 2010
Accepted 23 September 2010
Available online 7 October 2010

Keywords:
Silver(I) complexes
Hydrogen bonds
Sulfanylpropenoic acids
Mercaptopropenoic acids
X-ray structures

ABSTRACT

Compounds of the type [Ag(PPh$_3$)$_3$(HL)] {H$_2$***x***spa=3(aryl)-2-sulfanylpropenoic acids: ***x*** = ***Clp*** [3-(2-chlorophenyl)-], ***-o-mp*** [3-(2-methoxyphenyl)-], ***-p-mp*** [3-(4-methoxyphenyl)-], ***-o-hp*** [3-(2-hydroxyphenyl)-], ***-p-hp*** [3-(4-hydroxyphenyl-); H$_2$cpa = 2-cyclopentylidene-2-sulfanylacetic acid} were synthesized and characterised by IR and NMR (^{1}H ^{13}C and ^{31}P) spectroscopy and by FAB mass spectrometry. The crystal structures of [Ag(PPh$_3$)$_3$(HClpspa)], [Ag(PPh$_3$)$_3$(H-*o*-mpspa)], [Ag(PPh$_3$)$_3$(H-*p*-mpspa)] and [Ag(PPh$_3$)$_3$-(Hcpa)] reveal the presence of discrete molecular units containing an intramolecular O–H···S hydrogen bond between the S atom and one of the O atoms of the COOH group. This intramolecular hydrogen bond remains in [Ag(PPh$_3$)$_3$(H-*o*-hpspa)]·EtOH and [Ag(PPh$_3$)$_3$(H-*p*-hpspa)] but in both cases polymeric structures are built on the basis of O–H···O interactions that involve the –OH substituent of the phenyl group of the sulfanylpropenoate fragment.

1. Introduction

The biological activity and medicinal properties of silver [1,2] and gold [3,4] compounds, together with their technological applications [5,6], have brought about an increase in interest in the coordination chemistry of both elements [7].

In a search for new structural features of silver(I), we previously investigated [8] the reaction of this ion with PPh$_3$ and sulfanylcarboxylic acids such as R–CH=C(SH)–COOH, (hereafter H$_2$***x***spa). Whereas the usual proportion of Ag/PPh$_3$ in the synthesized solids was 1:1, a few crystals of [Ag(PPh$_3$)$_3$(Hfspa)] [H$_2$fspa = 3-(furyl)-2-sulfanylpropenoic acid] were isolated and these had a higher content of triphenylphosphine.

The synthesis of this type of compound was later optimised [9], enabling the preparation of the equivalent [Ag(PPh$_3$)$_3$(H***x***spa)] compounds for which H***x***spa are the phenyl- and thienylsulfanylpropenoic derivatives. The structure of [Ag(PPh$_3$)$_3$(Hpspa)] [H$_2$pspa = 3-(phenyl)-2-sulfanylpropenoic acid] was solved by X-ray diffraction.

The structures of the furyl- and phenyl-derivatives show that the Ag atom is bonded to three P atoms of three PPh$_3$ ligands and to the S atom of the monodeprotonated sulfanylcarboxylic acid (H***x***spa), in which the COOH group remains protonated. In other silver [8,9] or gold [10,11] compounds, such as [M(PPh$_3$)(H***x***spa)], with a lower content of triphenylphosphine, this COOH group participates in intermolecular hydrogen bonding with an equivalent group of a neighbouring molecule, thus affording the homosynthon carboxylic acid dimer. However, in the structures of [Ag(PPh$_3$)$_3$-(Hpspa)] and [Ag(PPh$_3$)$_3$(Hfspa)] the COOH group participates in an intramolecular O–H···S hydrogen bond with the metallated S atom to give isolated monomers, thus showing the prevalence of this bond over the carboxylic acid/dimer motif. Tiekink et al. previously showed for the specific case of (tricyclohexylphosphine)gold(I) 2-mercaptobenzoate that both structural motifs can be present and that the stability of one over the other is solvent-modulated [12,13].

In the study reported here we tried to ascertain whether the structural modification of the R-aryl group on the sulfanylcarboxylate ligand could modify the prevalence of the O–H···S hydrogen bond found for the phenyl- and the furyl-derivatives; in particular, we investigated whether new donor atoms or new substituents on the aryl ring could produce new synthons [14], thus changing the structure and the crystal packing of the prepared solids. We selected the ligands H$_2$***x***spa and H$_2$cpa (see Scheme 1) and prepared complexes of the type [Ag(PPh$_3$)$_3$(H***x***spa)]. The structures of [Ag(PPh$_3$)$_3$(HClpspa)], [Ag(PPh$_3$)$_3$(H-*o*-mpspa)], [Ag(PPh$_3$)$_3$-

* Corresponding author. Tel.: +34 981528074; fax: +34 981547102.
E-mail address: jose.sordo@usc.es (J. Sordo).

0277-5387/$ - see front matter © 2010 Elsevier Ltd. All rights reserved.
doi:10.1016/j.poly.2010.09.027

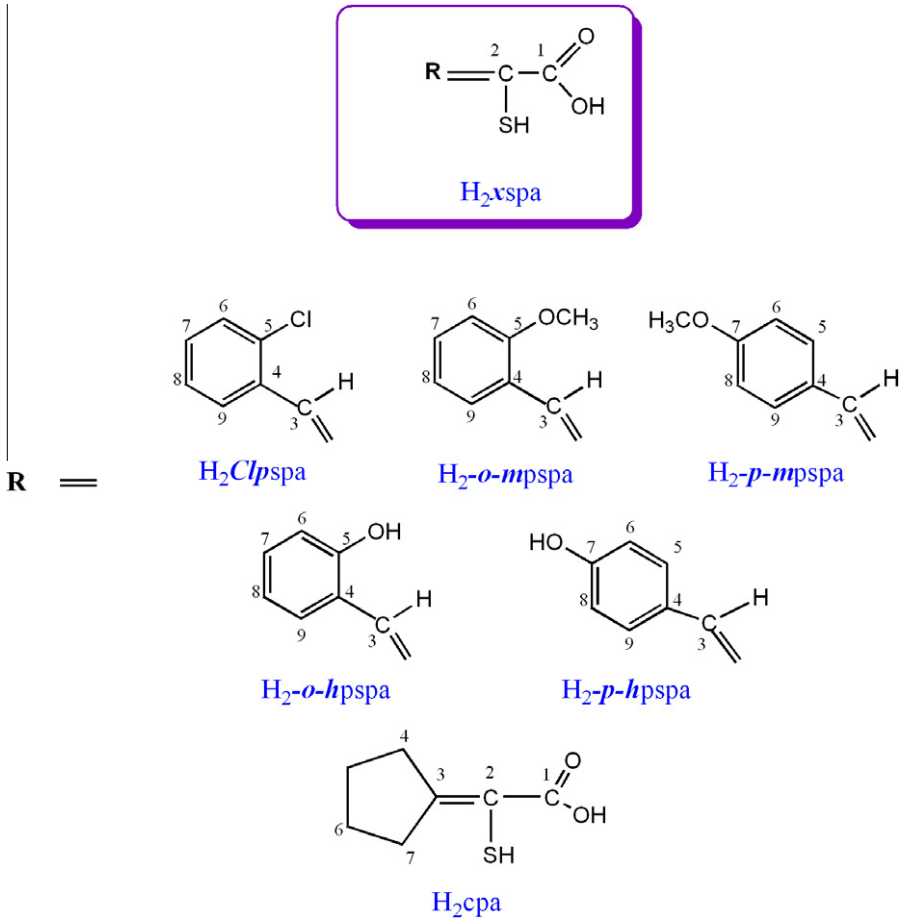

Scheme 1.

(H-*p*-mpspa)], [Ag(PPh$_3$)$_3$(Hcpa)], [Ag(PPh$_3$)$_3$(H-*o*-hpspa)]·EtOH and [Ag(PPh$_3$)$_3$(H-*p*-hpspa)] were solved by X-ray diffraction, with two types of structure found – one containing monomer units and the other containing hydrogen-bonded polymeric species.

2. Experimental

2.1. Materials and methods

2-Chlorobenzaldehyde, 2-methoxybenzaldehyde, 4-methoxybenzaldehyde, cyclopentanone, 2-hydroxybenzaldehyde and 4-hydroxybenzaldehyde (all from Aldrich), triphenylphosphine (Riedel-de-Haën) and silver nitrate (Prolabo) were all used as supplied. The 3-(2-aryl)-2-sulfanylpropenoic acids H$_2$Clpspa, H$_2$-*o*-mpspa, H$_2$-*p*-mpspa, H$_2$-*o*-hpspa and H$_2$-*p*-hpspa were prepared by condensation of the appropriate aldehyde with rhodanine [15], subsequent hydrolysis in an alkaline medium and acidification with aqueous HCl [16]. For the preparation of 2-cyclopentylidene-2-sulfanylacetic acid, (H$_2$cpa), a ketone (cyclopentanone) was used in the condensation reaction instead of an aldehyde [17]. Specific experimental conditions for H$_2$Clpspa, H$_2$-*o*-mpspa and H$_2$-*p*-mpspa were described in Ref. [8] and for H$_2$-*o*-hpspa and H$_2$-*p*-hpspa in Ref. [18].

[Ag(PPh$_3$)$_3$(NO$_3$)] was prepared according to the literature procedure [19].

Elemental analyses were performed on a Fisons 1108 microanalyser. Melting points were determined with a Büchi apparatus and are uncorrected. Mass spectra (MS) were recorded on a Kratos MS50TC spectrometer connected to a DS90 system and operating in FAB mode (*m*-nitrobenzyl alcohol, Xe, 8 eV; *ca.* 1.28×10^{-15} J); ions were identified by DS90 software and the data characterising the metallated peaks were calculated using the isotope ^{107}Ag. IR spectra (KBr pellets or Nujol mulls) were recorded on a Bruker IFS66 V FT-IR spectrophotometer and are reported in the synthesis section using the following abbreviations: vs = very strong, s = strong, m = medium, w = weak, sh = shoulder, br = broad. ^{1}H and ^{13}C NMR spectra were recorded in dmso-d_6 and/or CDCl$_3$ at room temperature on a Bruker AMX 300 spectrometer operating at 300.14 and 75.40 MHz, respectively, using 5 mm o.d. tubes; chemical shifts are reported relative to TMS using the solvent signals (δ ^{1}H = 2.50 ppm; δ ^{13}C = 39.5 ppm for dmso-d_6 and δ ^{1}H = 7.26 ppm; δ ^{13}C = 77.0 ppm in CDCl$_3$) as references. The splitting of proton resonances in the reported ^{1}H NMR spectra are defined as s = singlet, d = doublet, t = triplet, m = multiplet, *pst* = pseudotriplet and br = broad. ^{31}P NMR spectra were recorded in dmso-d_6 at 202.46 MHz on a Bruker AMX 500 spectrometer using 5 mm o.d. tubes and are reported relative to external neat H$_3$PO$_4$ (85%). All the physical measurements were carried out by the RIAIDT services of the University of Santiago de Compostela.

2.2. Synthesis of the complexes

The complexes [Ag(PPh$_3$)$_3$(H***x***spa)] and [Ag(PPh$_3$)$_3$(Hcpa)] were obtained by mixing a solution of the appropriate sulfanylcarboxylic acid in chloroform with a solution of [Ag(PPh$_3$)$_3$(NO$_3$)] and NaOAc in water. The mixture was shaken for 45 min, the organic phase was separated and dried with MgSO$_4$, and the CHCl$_3$ was evaporated under vacuum. The crude oily product was treated with 1:1

hexane/ethanol and the resulting solution was evaporated at room temperature.

*2.2.1. [Ag(PPh$_3$)$_3$(HClpspa)] (**1**)*

H_2Clpspa (0.05 g, 0.25 mmol), Ag(PPh$_3$)$_3$(NO$_3$) (0.23 g, 0.25 mmol), NaOAc (0.02 g, 0.25 mmol), $CHCl_3$ (15 cm^3), H_2O (25 cm^3), yellow crystals. Yield: 72%. M.p.: 158 °C. *Anal.* Calc. for $C_{63}H_{51}O_2SClP_3Ag$: C, 68.3; H, 4.7; S, 2.9. Found: C, 68.0; H, 5.0; S, 2.7%. MS (FAB): the main signals for metallated species are at *m*/*z* 1322 (2%), [M]$^+$; 953 (13), [(AgPPh$_3$)$_2$Clpspa]$^+$; 631 (100), [Ag(PPh$_3$)$_2$]$^+$ and 369 (54), [(AgPPh$_3$)]$^+$. IR (cm^{-1}): 1721 vs, ν(C=O); 1280 w, ν(C–O); 1480 s, 1435 vs, ν(PPh$_3$). NMR (DMSO-d_6): ^{1}H, δ 12.5 (s,br, 1H, C(1)OH), 7.86 (s, 1H, C(3)H), 7.54 (d, 1H, C(6)H), 7.09 (t, 1H, C(7)H), 7.15 (t, 1H, C(8)H), 9.46 (d, 1H, C(9)H), 7.23, 7.30, 7.40 (m, 45H, H(PPh$_3$)); ^{13}C, δ 171.4 C(1), 125.4 C(2), 132.0 C(3), 142.8 C(4), 135.5 C(5), 131.4 C(6), 131.6 C(7) 125.9 C(8), 127.7 C(9),133.2 (d, C$_o$(Ph$_3$), *J* = 16.8), 128.8 (d, C$_m$(Ph$_3$), *J* = 9.1), 129.8 C$_p$(Ph$_3$); ^{31}P {^{1}H}, δ 7.63 (s), 31.4 (s). NMR ($CDCl_3$): ^{1}H, δ 8.11 (s, 1H, C(3)H), 7.67 (d, 1H, C(6)H), 6.69 (t, 1H, C(7)H), 6.93 (t, 1H, C(8)H), 9.11 (d, 1H, C(9)H), 7.21, 7.26, 7.36 (m, 45H, H(PPh$_3$)). ^{13}C, δ 168.7 C(1), 125.5 C(2), 135.0 C(3), 138.4 C(4), 135.8 C(5), 130.2 C(6), 131.9 C(7) 127.8 C(8), 128.5 C(9),133.6 (d, C$_o$(Ph$_3$), *J* = 17.2), 128.8 (d, C$_m$(Ph$_3$), J = 9.5), 129.7 C$_p$(Ph$_3$).

*2.2.2. [Ag(PPh$_3$)$_3$(H-o-mpspa)] (**2**)*

H_2-*o*-mpspa (0.11 g, 0.52 mmol), Ag(PPh$_3$)$_3$(NO$_3$) (0.5 g, 0.52 mmol), NaOAc (0.07 g, 0.84 mmol), $CHCl_3$ (20 cm^3), H_2O (30 cm^3), yellow crystals. Yield 87%. M.p.: 166 °C. *Anal.* Calc. for $C_{64}H_{54}O_3SP_3Ag$: C, 69.6; H, 4.7; S, 2.9. Found: C, 69.7; H, 5.0; S, 2.9%. MS (FAB): the main signals for metallated species are at *m*/*z* 1319 (7%), [M]$^+$; 949 (2), [(AgPPh$_3$)$_2$-*o*-mpspa]$^+$; 631 (100), [Ag(PPh$_3$)$_2$]$^+$ and 369 (60), [(AgPPh$_3$)]$^+$. IR (cm^{-1}): 1715 vs, ν(C=O); 1241 m, ν(C–O); 2836 w, ν_s(OCH$_3$); 1479s, 1434 vs, ν(PPh$_3$). NMR (DMSO-d_6): ^{1}H, δ 7.93 (s, 1H, C(3)H), 9.21 (d, 1H, C(6)H), 6.71 (t, 1H, C(7)H), 7.16 (*p*st, 1H, C(8)H), 6.91 (d, 1H, C(9)H), 3.73 (s, 3H, OCH$_3$), 7.23, 7.32, 7.41, 7.61 (m, 45H, H(PPh$_3$)); ^{13}C, δ 172.0 C(1), 128.3 C(2), 133.2 C(3), 126.4 C(4), 156.8 C(5), 110.3 C(6), 129.3 C(7), 119.3 C(8), 128.8 C(9), 55.4 C(OCH$_3$), 133.3 (d, C$_o$(Ph$_3$), *J* = 18.3), 128.9 (d, C$_m$(Ph$_3$), *J* = 7.6), 129.9 C$_p$(Ph$_3$); ^{31}P {^{1}H}, δ 8.7 (s), 31.5 (s).

*2.2.3. [Ag(PPh$_3$)$_3$(H-p-mpspa)] (**3**)*

H_2-*p*-mpspa (0.05 g, 0.24 mmol), Ag(PPh$_3$)$_3$(NO$_3$) (0.23 g, 0.24 mmol), NaOAc (0.02 g, 0.24 mmol), $CHCl_3$ (10 cm^3), H_2O (20 cm^3), yellow crystals. Yield 81%. M.p.: 161 °C. *Anal.* Calc. for $C_{64}H_{54}O_3SP_3Ag$: C, 69.6; H, 4.7; S, 2.9. Found: C, 69.3; H, 5.0; S, 2.7%. MS (FAB): the main signals for metallated species are at *m*/*z* 1319 (2%), [M]$^+$; 949 (13), [(AgPPh$_3$)$_2$-*p*-mpspa]$^+$; 631 (100), [Ag(PPh$_3$)$_2$]$^+$ and 369 (54), [(AgPPh$_3$)]$^+$. IR (cm^{-1}): 1715 vs, ν(C=O); 1252 s, ν(C–O); 2835 w, ν_s(OCH$_3$); 1479 s, 1434 vs, ν(PPh$_3$). NMR (DMSO-d_6): ^{1}H, δ 12.30 (s,br, 1H, C(1)OH), 7.54 (s, 1H, C(3)H), 8.26 (d, 2H, C(5)H, C(9)H), 6.71 (d, 2H, C(6)H, C(8)H), 3.71 (s, 3H, OCH$_3$), 7.20, 7.29, 7.38 (m, 45H, H(PPh$_3$)); ^{13}C, δ 171.5 C(1), 128.6 C(2), 132.1 C(3), 130.5 C(4), 132.0 C(5) and C(9), 112.9 C(6) and C(8), 158.1 C(7), 54.9 C(OCH$_3$), 133.3 (d, C$_o$(Ph$_3$), *J* = 16.8), 128.8 (d, C$_m$(Ph$_3$), *J* = 7.6), 129.8 C$_p$(Ph$_3$); ^{31}P {^{1}H}, δ 9.0 (s), 31.5 (s).

*2.2.4. [Ag(PPh$_3$)$_3$(Hcpa)] (**4**)*

H_2cpa (0.04 g, 0.25 mmol), Ag(PPh$_3$)$_3$(NO$_3$) (0.25 g, 0.25 mmol), NaOAc (0.025 g, 0.30 mmol), $CHCl_3$ (12 cm^3), H_2O (25 cm^3), brown crystals. Yield 86%. M.p.: 165 °C. *Anal.* Calc. for $C_{61}H_{54}O_2SP_3Ag$: C, 69.6; H, 5.2; S, 3.1. Found: C, 69.5; H, 5.2; S, 3.0%. MS (FAB): the main signals for metallated species are at *m*/*z* 1265 (2%), [M]$^+$; 987 (16), [(AgPPh$_3$)$_2$cpa]$^+$; 631(100), [Ag(PPh$_3$)$_2$]$^+$ and 369 (77), [(AgPPh$_3$)]$^+$. IR (cm^{-1}): 1714 vs ν(C=O); 1479 s, 1434 vs, ν(PPh$_3$); 2862 m, ν_s(CH$_2$); 2949 m, ν_a(CH$_2$). NMR (DMSO-d_6): ^{1}H, δ 12.00 (s,br, 1H, C(1)OH), 2.41 (m, 2H, C(4)H$_2$), 1.34 (m, 2H, C(5)H$_2$), 1.23 (m, 2H, C(6)H$_2$), 2.33 (m, 2H, C(7)H$_2$), 7.23, 7.35, 7.39, 7.58 (m, 45H, H(PPh$_3$)); ^{13}C, δ 170.1 C(1), 123.6 C(2), 156.4 C(3), 37.8 C(4), 27.3 C(5), 25.0 C(6), 34.9 C(7), 133.3 (d, C$_o$(Ph$_3$), *J* = 18.3), 128.9 (d, C$_m$(Ph$_3$), *J* = 7.6), 129.7 C$_p$(Ph$_3$); ^{31}P {^{1}H}, δ 5.3 (s), 31.5 (s).

*2.2.5. [Ag(PPh$_3$)$_3$(H-o-hpspa)]·EtOH (**5**)*

H_2-*o*-hpspa (0.045 g, 0.23 mmol), Ag(PPh$_3$)$_3$(NO$_3$) (0.2 g, 0.23 mmol), NaOAc (0.02 g, 0.23 mmol), $CHCl_3$ (10 cm^3), H_2O (20 cm^3), orange crystals. M.p.: 95 °C. *Anal.* Calc. for $C_{65}H_{58}O_4SP_3Ag$: C, 68.7; H, 5.1; S, 2.8. Found: C, 69.0; H, 4.9; S, 3.0%. MS (FAB): the main metallated signals are at *m*/*z* 935 (3%), [(AgPPh$_3$)$_2$-*o*-hpspa]$^+$; 631 (100), [Ag(PPh$_3$)$_2$]$^+$ and 369 (58), [(AgPPh$_3$)]$^+$. IR (cm^{-1}): 1719 vs, ν(C=O); 1222 m/1268 m, ν(C–O); 1479 vs, 1434 vs, ν(PPh$_3$). NMR (DMSO-d_6): ^{1}H, δ 12.50 (s,br, 1H, C(1)OH), 7.95 (s, 1H, C(3)H), 9.54 (s, 1H, C(5)OH), 6.79 (d, 1H, C(6)H), 7.00 (*p*st, 1H, C(7)H), 6.95 (t, 1H, C(8)H), 8.97 (d, 1H, C(9)H), 7.23, 7.33, 7.58 (m, 45H, H(PPh$_3$)); ^{13}C, δ 172.0 C(1), 128.7 C(3), 134.3 C(4), 155.3 C(5), 115.0 C(6), 128.3 C(7) 118.0 C(8), 133.2 (d, C$_o$(Ph$_3$), *J* = 16.8), 128.8 (d, C$_m$(Ph$_3$), *J* = 7.6), 129.7 C$_p$(Ph$_3$); ^{31}P {^{1}H}, δ 6.2 (s), 31.5 (s).

*2.2.6. [Ag(PPh$_3$)$_3$(H-p-hpspa)] (**6**)*

H_2-p-hpspa (0.045 g, 0.23 mmol), Ag(PPh$_3$)$_3$(NO$_3$) (0.2 g, 0.23 mmol), NaOAc (0.02 g, 0.23 mmol), $CHCl_3$ (10 cm^3), H_2O (20 cm^3), yellow crystals. Yield 78%. M.p.: 157 °C. *Anal.* Calc. for $C_{63}H_{52}O_3SP_3Ag$: C, 69.5; H, 4.7; S, 2.9. Found: C, 69.3; H, 4.9; S, 2.7%. MS (FAB): the main signals for metallated species are at *m*/*z* 1305 (2%), [M]$^+$; 935 (8), [(AgPPh$_3$)$_2$-*p*-hpspa]$^+$; 631 (100), [Ag(PPh$_3$)$_2$]$^+$ and 369 (79), [(AgPPh$_3$)]$^+$. IR (cm^{-1}): 1718 vs, ν(C=O); 1223 m/1268 m, ν(C–O); 1479 s, 1434 vs, ν(PPh$_3$). NMR (DMSO-d_6): ^{1}H, δ 8.12 (d, 2H, C(5)H, C(9)H), 6.66 (d, 2H, C(6)H, C(8)H), 9.63 (s,br, 1H, C(7)OH), 7.25, 7.34, 7.42, 7.62 (m, 46H, C(3)H, H(PPh$_3$)); ^{13}C, δ 171.8 C(1), 115.8 C(2), 125.9 C(3), 137.1 C(4), 129.6 C(5) and C(9), 114.5 C(6) and C(8), 156.7 C(7), 133.3 (d, C$_o$(Ph$_3$), *J* = 18.3), 128.8 (d, C$_m$(Ph$_3$), *J* = 9.1), 129.8 C$_p$(Ph$_3$); ^{31}P {^{1}H}, δ 8.5 (s), 31.5 (s).

2.3. Crystallography

2.3.1. X-ray data collection and reduction

Single crystals of [Ag(PPh$_3$)$_3$(HClpspa)] (**1**), [Ag(PPh$_3$)$_3$(H-*o*-mpspa)] (**2**), [Ag(PPh$_3$)$_3$(H-*p*-mpspa)] (**3**), [Ag(PPh$_3$)$_3$(Hcpa)] (**4**), [Ag(PPh$_3$)$_3$(H-*o*-hpspa)]·EtOH (**5**) and [Ag(PPh$_3$)$_3$(H-*p*-hpspa)] (**6**) were mounted on glass fibres for data collection in a Bruker Smart CCD automatic diffractometer at 293 K using Mo Kα radiation (λ = 0.71073 Å).

All crystallographic data were corrected for Lorentz and polarisation effects using SAINT [20] and multiscan absorption corrections were applied using SADABS [21]. The structures were solved by direct methods and refined by full-matrix least squares on F^2 using SHELX97 [22]. All non-H atoms were refined anisotropically. H atoms were placed at their ideal positions and refined as riders – except for the carboxyl hydrogen atoms bound to O(1), which were refined isotropically. Graphics were produced with *PLATON* and *MERCURY* [23]. The crystal data, experimental details and refinement results are summarized in Table 1.

The methylene C(6) group of the cyclopentanone fragment in **4** is affected by disorder. The disorder was modelled by the refinement of the occupancy factor of two equivalent groups, which converged to values close to 50%. This value was fixed in the last stage of the refinement.

Table 1
Crystal data for [Ag(PPh$_3$)$_3$(HClpspa)] (**1**), [Ag(PPh$_3$)$_3$(H-*o*-mpspa)] (**2**), [Ag(PPh$_3$)$_3$(H-*p*-mpspa)] (**3**), [Ag(PPh$_3$)$_3$(Hcpa)] (**4**), [Ag(PPh$_3$)$_3$(H-*o*-hpspa)]·EtOH (**5**) and [Ag(PPh$_3$)$_3$(H-*p*-hpspa)] (**6**).

Compound	[Ag(PPh$_3$)$_3$(HClpspa)] (**1**)	[Ag(PPh$_3$)$_3$(H-*o*-mpspa)] (**2**)	[Ag(PPh$_3$)$_3$(H-*p*-mpspa)] (**3**)	[Ag(PPh$_3$)$_3$(Hcpa)] (**4**)	[Ag(PPh$_3$)$_3$(H-*o*-hpspa)]·EtOH (**5**)	[Ag(PPh$_3$)$_3$(H-*p*-hpspa)] (**6**)
Empirical formula	$C_{63}H_{51}AgClO_2P_3S$	$C_{64}H_{54}AgO_3P_3S$	$C_{64}H_{54}AgO_3P_3S$	$C_{61}H_{54}AgO_2P_3S$	$C_{65}H_{58}AgO_4P_3S$	$C_{63}H_{52}AgO_3P_3S$
M	1108.33	1103.91	1103.91	1051.88	1135.95	1089.89
Crystal system	triclinic	triclinic	monoclinic	triclinic	monoclinic	monoclinic
Space group	*P*1	$P\bar{1}$	*P*2(1)/c	$P\bar{1}$	*P*2(1)/c	*P*n
a (Å)	11.5572(8)	12.6746(11)	13.9439(8)	13.4899(10)	17.869(2)	12.1826(11)
b (Å)	11.8894(8)	12.8038(11)	14.2274(8)	13.7625(10)	14.0708(15)	13.1205(12)
c (Å)	12.5549(8)	18.9780(15)	27.3290(16)	14.2879(11)	25.1300(18)	16.9022(15)
α (°)	105.4010(10)	89.482(2)	90	79.58(2)	90	90
β (°)	108.0270(10)	88.158(2)	94.7890(10)	89.744(2)	117.555(5)	96.647(2)
γ (°)	109.5150(10)	61.678(2)	90	86.997(2)	90	90
V (Å^3)	1409.14(16)	2709.7(4)	5402.7(5)	2604.9(4)	5601.7(10)	2683.5(4)
Z	1	2	4	2	4	2
$D_{calc.}$ (Mg/m^3)	1.306	1.353	1.357	1.340	1.347	1.349
M (mm^{-1})	0.569	0.545	0.547	0.562	0.531	0.550
Crystal size (mm^3)	0.38 × 0.27 × 0.07	0.26 × 0.23 × 0.15	0.05 × 0.21 × 0.36	0.20 × 0.16 × 0.10	0.26 × 0.14 × 0.12	0.30 × 0.20 × 0.19
θ Range for data collection (°)	1.87–28.02	1.81–28.10	1.47–28.17	1.45–28.05	1.68–28.04	1.55–28.07
Index ranges	$-13 \leqslant h \leqslant 15 - 13 \leqslant k \leqslant 15$ $-16 \leqslant l \leqslant 13$	$-16 \leqslant h \leqslant 16$ $-16 \leqslant k \leqslant 16$, $-25 \leqslant l \leqslant 16$	$-18 \leqslant h \leqslant 18$, $-18 \leqslant k \leqslant 18$, $-36 \leqslant l \leqslant 20$	$-17 \leqslant h \leqslant 17$, $-16 \leqslant k \leqslant 18$, $-13 \leqslant l \leqslant 18$	$-23 \leqslant h \leqslant 15$ $-17 \leqslant k \leqslant 18$ $-32 \leqslant l \leqslant 33$	$-16 \leqslant h \leqslant 16$ $-16 \leqslant k \leqslant 17$ $-16 \leqslant l \leqslant 22$
Reflections collected	9169	15893	29166	14281	27587	15840
Unique reflections, *R*	7558[*R*(int) = 0.0202]	11111[*R*(int) = 0.0685]	12047 [*R*(int) = 0.0681]	9996[*R*(int) = 0.0557]	12042[*R*(int) = 0.1179]	9022[*R*(int) = 0.0827]
Final R_1, wR_2 [$I > 2\sigma(I)$]	0.0474, 0.1275	0.0567, 0.0841	0.0524, 0.0841	0.0488, 0.0673	0.0445, 0.0535	0.0440, 0.0562
Final *R* indices (all data)	0.0568, 0.1328	0.1310, 0.0994	0.1732, 0.1039	0.1969, 0.0873	0.2982, 0.0931	0.1087, 0.0695
Largest diff. peak and hole (e.Å^{-3})	1.085 and –0.719	0.730 and –0.908	0.990 and –0.445	0.425 and –0.281	0.332 and –0.343	0.480 and –0.340
Flack parameter	–0.02(2)					

3. Results and discussion

3.1. Synthesis

The synthesis of the complexes was carried out in a heterogeneous medium (chloroform/water) by using the appropriate H_2L ligand, [Ag(PPh$_3$)$_3$(NO$_3$)] and NaOAc. The crude, oily product obtained after agitation, separation and drying of the organic phase and the elimination of the organic solvent was treated with 1:1 hexane/ethanol. The resulting solution was evaporated at room temperature. As well as the $[M]^+$ peak, the FAB^+ mass spectra of the compounds all show signals for fragments with different PPh_3 contents, which implies easy cleavage of the Ag–P bonds. Some cleavage of the Ag–S bonds was also evident.

3.2. Spectroscopy

The IR spectra of the complexes are all similar and provide evidence for deprotonation of the SH group in all cases due to the absence of a ν(SH) band, which is located near to 2565 cm^{-1} in the spectra of the free ligands. Furthermore, the positions of the COOH vibrations are slightly shifted with respect to the position in the spectra of the free ligands and δ(OH) in the complexes overlaps the PPh_3 vibrations.

The ^{1}H NMR spectra do not contain any SH signal and the presence of a signal at about 12.5 ppm is attributable to the COOH group. In the ^{13}C NMR spectra the shift of the C(3) signals to higher field is in keeping with the persistence of the S-coordination observed in the solid state [8–10]. The C(1) signal lies at positions close to those previously found in the spectra of equivalent sulfanylpropenoato complexes [8,9] and in [Ag(PPh$_3$)$_3$(Hmna)] (H_2mna = 2-sulfanylnicotinic acid) [24] and [Ag(PPh$_3$)$_3$(Hmba)]

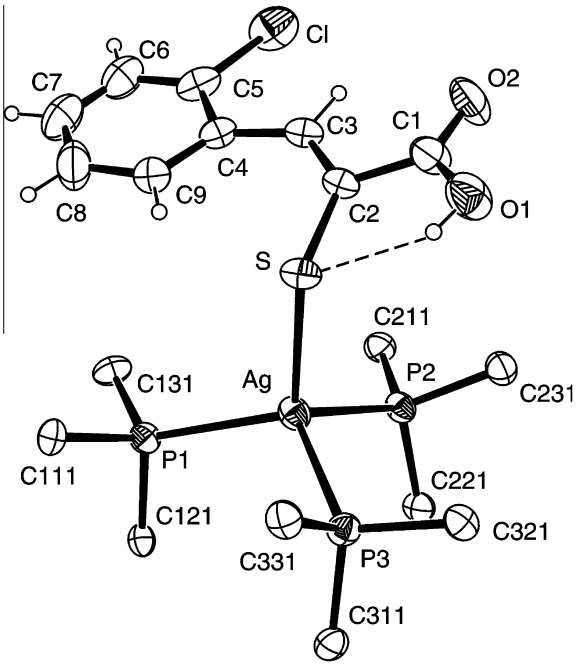

Fig. 1. The crystal structure of [Ag(PPh$_3$)$_3$(HClpspa)] (**1**) together with the numbering scheme (for clarity only the C_{ipso} of the phenyl triphenylphosphine ring is indicated).

(H_2mba = 2-sulfanylbenzoic acid) [25]. The room temperature $^{31}P\{1H\}$ NMR spectra show a singlet at 5.3–9.0 ppm and this is due to the coordinated PPh_3 ligand; a weak singlet near to 31.5 ppm indicates the formation of triphenylphosphine oxide [26] generated by the oxidation of some of the released triphenylphosphine. The same phenomenon was previously found for $[Ag(PPh_3)_3(Hfspa)]$ [9].

3.3. X-ray studies

3.3.1. Molecular structure

The Ag atom in **1** (Fig. 1) is coordinated to three P atoms from three PPh_3 ligands and to the S atom of the HClpspa moiety, with the angles (Table 2) around the silver atom showing that the coordination polyhedron can be described as a distorted

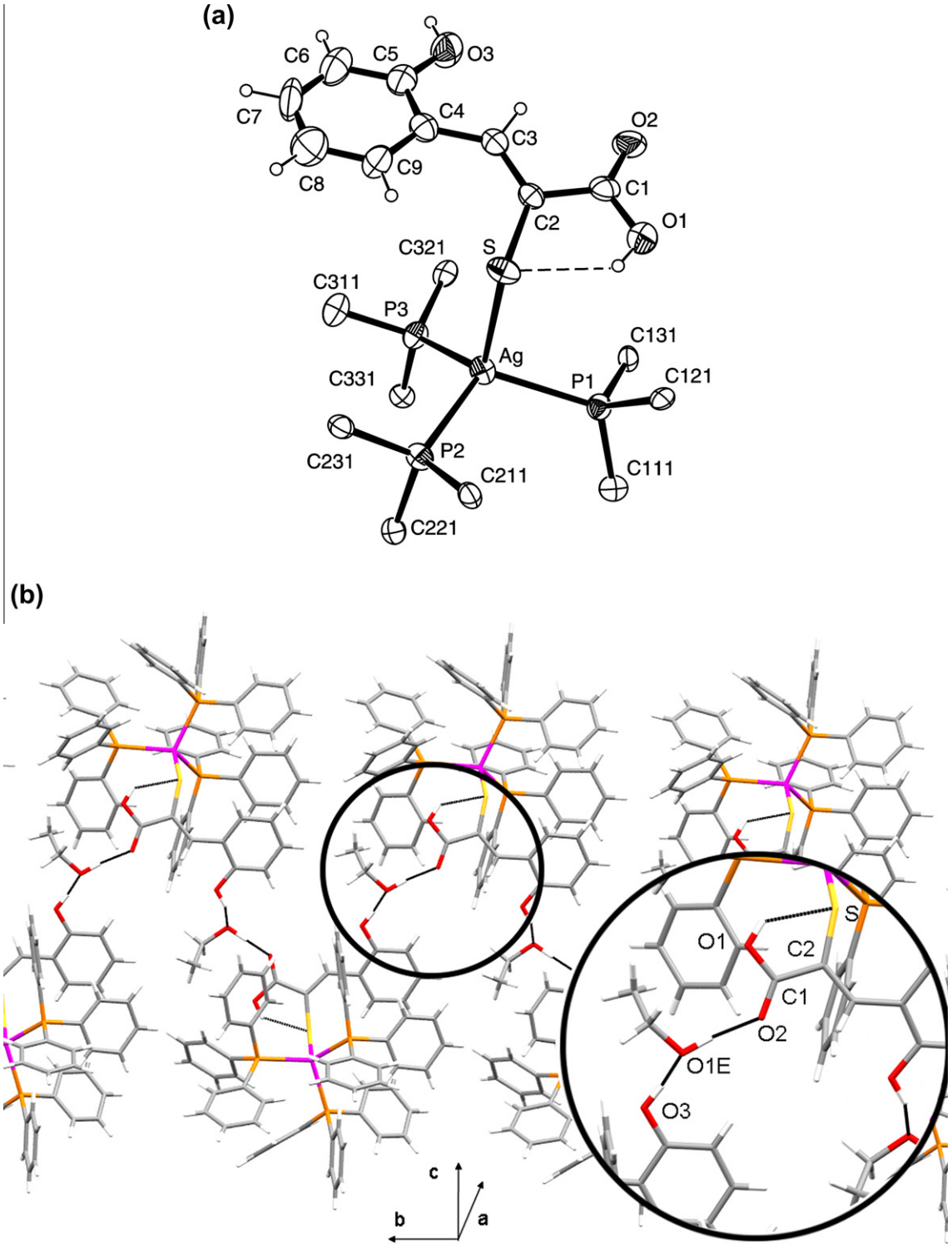

Fig. 2. (a) The crystal structure of $[Ag(PPh_3)_3(H\text{-}o\text{-}hpspa)]\cdot CH_3OH$ (**5**) (the phenylphosphine ring and the methanol molecule have been omitted). (b) A view of the crystal structure of (**5**).

tetrahedron. Similar distorted $AgSP_3$ kernels are present in **2**–**4**, (Table 2; Figs. S1–S3), [$Ag(PPh_3)_3$(Hfspa)] [8] [H_2fspa = 3-(2-furyl)-2-sulfanylpropenoic acid], [$Ag(PPh_3)_3$(Hpspa)] [9], [$Ag(PPh_3)_3$-(Hmna)] [24], [$Ag(PPh_3)_3$(Hmba)] [25], [$Ag(PPh_3)_3(L_a)$] [L_a = 4-(methylthio)-2-thioxo-1,3-dithiole-2-thiolate] [27] and [Ag-$(PPh_3)_3$ (L_b)] [L_b = 1,2-dicyano-1-(methylthio)ethene-2-thiolate] [27]. In these complexes the structural parameters of the kernel do not differ significantly; the Ag–S distance ranges from 2.5766(16) Å in **4** to 2.6524(17) in **1** and the Ag–P distance ranges from 2.5164(12) Å in **2** to 2.6495(8)Å in the L_a derivative. The angles around the metal range from 95.89(4) to 121.82(4)° in the most distorted structure (the L_b derivative) and from 103.68(3)° to 116.23(3)° in the least distorted ([$Ag(PPh_3)_3$(Hfspa)]). The Hpspa and Hmna derivatives are also only slightly distorted.

Another common structural feature is the intramolecular hydrogen bond between the COOH group and the S atom. The geometrical parameters of this bond are shown in Table 3; the values are all similar to each other and also to those previously described for [$Ag(PPh_3)_3$(Hfspa)] [8] and [$Ag(PPh_3)_3$(Hpspa)] [9]. These parameters can be compared with those of thioxoketones [28–30] but a more relevant comparison can be made with the O–H···S intramolecular hydrogen bond present in 3-thioxo-2-pyridinecarboxylic acid [30,31] or with that present in some forms of [$Au(Pcy_3)$(2-Hmba)] [13]. These latter compounds contain a –C(S)–CH–COOH fragment instead of C(S)–COOH, but in all cases a COOH group and an S atom are involved and similar S···O distances, slightly longer S···H distances and narrower O–H···S angles are found in the complexes reported here. The formation of this intramolecular bond is possible due to (or the bond is responsible for) the appropriate position of the COOH group with respect to the S atom. For the complexes included in this paper, the angle between the S–C(2)–C(3)–C(4) and the C(1)–O(1)–O(2) planes range from 11(2)° in **1** to 3(2)° in **4**.

3.3.2. Crystal packing

Compounds **1**–**4** consist of discrete molecular units that are packed by very weak C–H···O and C–H···π interactions. In compound **1**, the asymmetric molecules of [$Ag(PPh_3)_3$(HClpspa)], in a

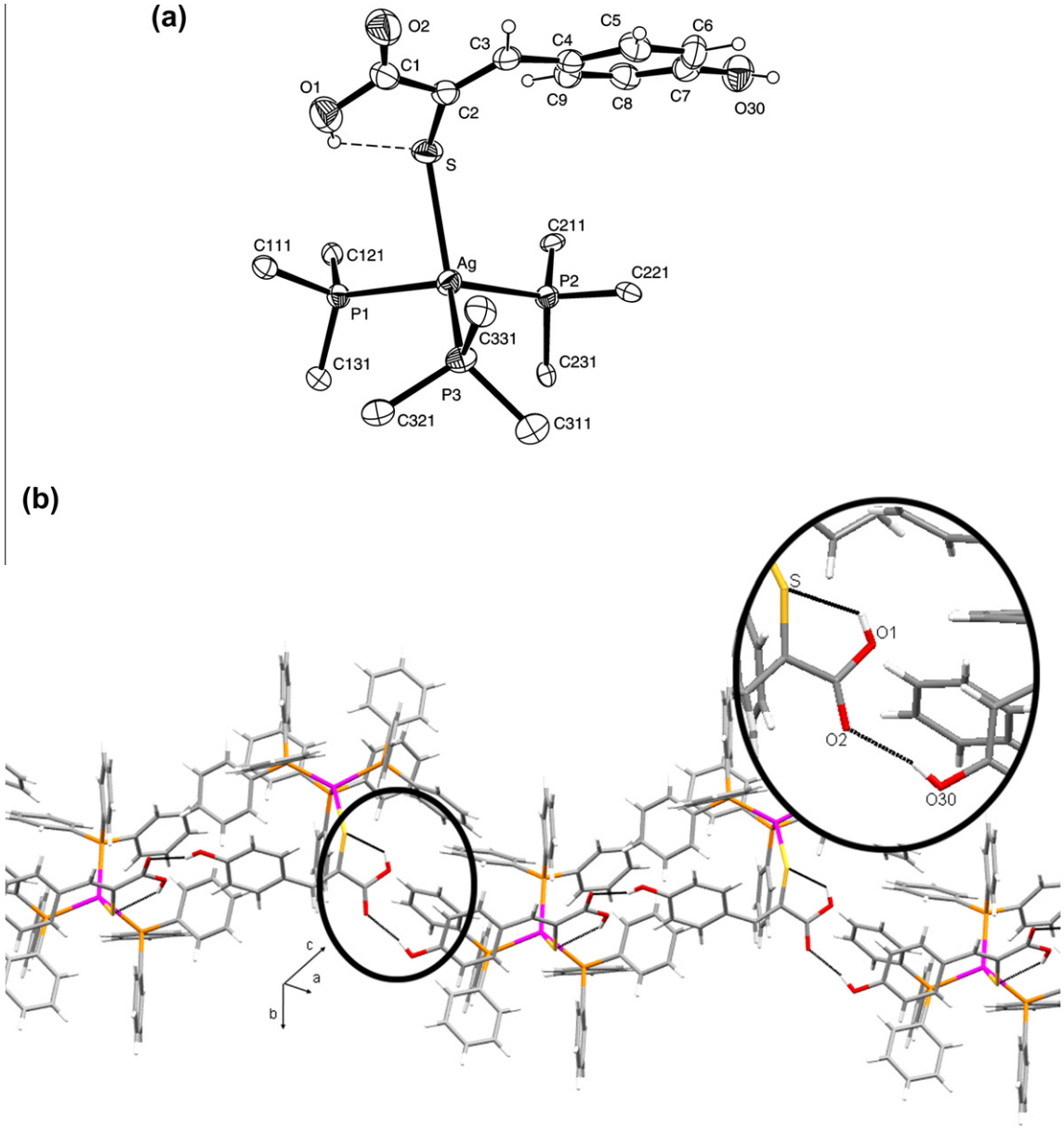

Fig. 3. (a) The crystal structure of [$Ag(PPh_3)_3$(H-*p*-hpspa)] (**6**) together with the numbering scheme. (b) A view of the polymeric structure of (**6**).

Table 2
Selected interatomic distances (Å) and angles (°) for complexes [Ag(PPh_3)$_3$(HClpspa)] (**1**), [Ag(PPh_3)$_3$(H-*o*-mpspa)] (**2**), [Ag(PPh_3)$_3$(H-*p*-mpspa)] (**3**), [Ag(PPh_3)$_3$(Hcpa)] (**4**), [Ag(PPh_3)$_3$(H-*o*-hpspa)].EtOH (**5**) and [Ag(PPh_3)$_3$(H-*p*-hpspa)] (**6**).

	1	**2**	**3**	**4**	**5**	**6**
(*a*) *Ag environment*						
Ag–P(2)	2.5438(17)	2.5915(12)	2.5533(12)	2.5614(18)	2.5710(18)	2.5363(18)
Ag–P(1)	2.5792(19)	2.6224(12)	2.6433(12)	2.5829(16)	2.5800(17)	2.5995(18)
Ag–P(3)	2.6403(16)	2.5164(12)	2.5994(11)	2.6300(17)	2.5657(19)	2.5351(16)
Ag–S	2.6524(17)	2.6241(12)	2.6062(13)	2.5766(16)	2.6692(15)	2.6311(17)
P(2)–Ag–P(1)	115.51(5)	108.33(4)	111.23(4)	112.11(6)	112.26(6)	113.12(5)
P(2)–Ag–P(3)	109.03(6)	112.44(4)	114.75(4)	112.38(5)	111.48(6)	110.52(6)
P(1)–Ag–P(3)	112.14(6)	116.00(4)	110.71(4)	110.09(5)	116.21(6)	114.75(6)
P(2)–Ag–S	111.69(6)	95.26(4)	115.52(4)	113.75(6)	100.43(6)	104.90(6)
P(1)–Ag–S	110.15(6)	106.55(4)	104.23(4)	108.70(6)	102.20(6)	88.23(5)
P(3)–Ag–S	96.79(5)	116.12(4)	99.42(4)	99.05(6)	112.79(6)	123.54(6)
(*b*) *H_2**x**spa*						
O(1)–C(1)	1.348(11)	1.328(5)	1.308(8)	1.341(9)	1.329(7)	1.323(7)
O(2)–C(1)	1.208(11)	1.191(5)	1.160(6)	1.159(9)	1.191(7)	1.204(7)
C(1)–C(2)	1.486(12)	1.518(6)	1.535(8)	1.513(10)	1.501(9)	1.503(9)
C(2)–C(3)	1.360(10)	1.342(5)	1.378(7)	1.363(8)	1.375(7)	1.350(7)
C(3)–C(4)	1.477(11)	1.457(6)	1.472(7)	1.524(8)	1.458(8)	1.458(8)
O(1)–C(1)–O(2)	119.0(9)	119.5(5)	118.9(8)	120.3(9)	125.8(8)	118.8(7)
O(1)–C(1)–C(2)	114.6(8)	114.5(4)	113.9(7)	108.8(8)	113.4(7)	114.9(6)
O(2)–C(1)–C(2)	126.4(8)	126.0(5)	127.1(7)	131.0(9)	125.8(8)	126.2(7)
C(3)–C(2)–C(1)	112.5(7)	114.7(4)	112.9(5)	115.5(7)	113.4(6)	116.2(6)
C(3)–C(2)–S	131.2(6)	129.6(4)	128.0(5)	124.5(6)	128.9(6)	127.7(5)
C(1)–C(2)–S	116.2(5)	115.5(3)	119.2(5)	119.9(6)	117.7(5)	116.1(5)

conformational enantiomer, are packed in the non-centrosymmetric space group *P*1 (No. 1). The intermolecular interactions are likely able to induce head-to-head aggregates in compounds **2**–**4** and, consequently, both conformational enantiomers are present in centrosymmetric (achiral) crystals. In contrast, [Ag(PPh_3)$_3$(H-*o*-hpspa)]·EtOH (**5**) and [Ag(PPh_3)$_3$(H-*p*-hpspa)] (**6**) contain an additional OH group that can participate in intermolecular hydrogen bonding to form polymeric structures.

The structures of the Ag(PPh_3)$_3$(H-*o*-hpspa) and Ag(PPh_3)$_3$(H-*p*-hpspa) units present in **5** and **6** are respectively shown in Figs. 2a and 3a and selected bond distances and angles for these compounds are given in Table 2. Note the presence in **6** of two shorter Ag–P bond distances and the narrowest and the widest tetrahedral angles of the compounds described in this paper. The CO_2H group in **5** is involved in the intramolecular O–H···hydrogen bond and in an intermolecular hydrogen bond. In the latter interaction, the O(2) atom of the carboxylic acid group and the OH group of the ethanol molecule are involved in a moderate hydrogen bond [O(1E)–H(1E)···O(2) = 0.97, 1.97, 2.717(6) Å, 132.3°]. Besides, the O atom also behaves as a hydrogen bond acceptor with the –OH group of the phenyl ring of the H-*o*-hpspa ligand [O(3)–H(3)···(1E)$^{\#1}$ = 0.843(5), 2.018(3), 2.685(6) Å, 135.4(4)°; #1 = $-x$, $y+1/2, -z-1/2$]. On the basis of these two bonds, each ethanol molecule bridges two neighbouring [Ag(PPh_3)$_3$(H-*o*-hpspa)] units to give rise to chains running along the *b* axis, as depicted in Fig. 2b.

The orientation of the OH group in the phenyl ring of the H-*p*-hpspa ligand allows this kind of interaction to be established directly between the molecules of **6** through hydrogen bonding between the former group and the carboxylic acid oxygen [O(30)–H(30)···O(2)$^{\#1}$ = 0.82, 1.98, 2.777(6) Å, 163.3°], #1 = $x-1/2$, $-y+1$, $z-1/2$, a situation that results in chains as shown in Fig. 3b.

The structural parameters of the O–H···O hydrogen bond present in **5** and **6**, when compared with those described previously for systems in which equivalent –OH groups were involved [32,33], reveal longer O···O distances and narrower O–H···O angles in this case. As far as the structural parameters of the COOH group are concerned, differences can be observed that are related with the type of hydrogen bond in which the group is involved. More marked differences between the two C–O distances are observed when the group is involved in the O–H···S intramolecular hydrogen bond and less marked differences are found in **5**, **6** and other complexes in which the carboxylic acid dimer synthon is present [10–13].

Table 3
Structural parameters involved in the intramolecular hydrogen bond O–H···*S* present in [Ag(PPh_3)$_3$(HL)] complexes.

Compound	*d*(O–H)	*d*(H···S)	*d*(O···S)	<(OHS)	Angle (°) between the planes C(1)–O(1)–O(2)/S–C(2)–C(3)–C(4)
(**1**)	0.82	2.26	2.851(7)	129.6	11(2)
(**2**)	0.84	2.23	2.848(3)	130.5	8.0(6)
(**3**)	0.67(6)	2.38(7)	2.924(7)	139(9)	3.7(9)
(**4**)	0.841(8)	2.1819(18)	2.834(7)	134.4(4)	3(2)
(**5**)	0.82	2.25	2.858(5)	130.8	5.8(3)
(**6**)	0.82	2.25	2.853(5)	130.1	6.7(8)

4. Conclusions

The synthesis and the structural study of complexes of the type [Ag(PPh_3)$_3$(H**x**spa)] [where H_2**x**spa = R–CH=C(SH)–COOH] and [Ag(PPh_3)$_3$(Hcpa)] [where H_2cpa = C_5H_8=C(SH)–COOH] enabled the identification of two classes of structures. One type of structure is present in [Ag(PPh_3)$_3$(HClpspa)] (**1**), [Ag(PPh_3)$_3$(H-*o*-mpspa)] (**2**), [Ag(PPh_3)$_3$(H-*p*-mpspa)] (**3**) and [Ag(PPh_3)$_3$(Hcpa)] (**4**) and this contains an intramolecular O–H···S hydrogen bond between the S atom and one of the O atoms of the COOH group. The introduction of –OH substituents in the phenyl ring in [Ag(PPh_3)$_3$(H-*o*-hpspa)]·EtOH (**5**·EtOH) and [Ag(PPh_3)$_3$(H-*p*-hpspa)] (**6**) leads to the formation of an intermolecular O–H···O hydrogen bond involving the new –OH group and one of the O atoms of the COOH group. The formation of this bond gives rise to polymeric structures and is

compatible with the presence of the O–H···S intramolecular hydrogen bond, which is also present in these compounds.

Acknowledgements

We thank the Spanish Ministry of Science and Technology for financial support under projects BQU2002-04524-C02-01 and BQU2002-04524C02-02.

Appendix A. Supplementary data

CCDC 785399, 785400, 785401, 785402, 785403 and 785404 contain the supplementary crystallographic data for this paper. These data can be obtained free of charge via http://www.ccdc.cam.ac.uk/conts/retrieving.html, or from the Cambridge Crystallographic Data Centre, 12 Union Road, Cambridge CB2 1EZ, UK; fax: (+44) 1223-336-033; or e-mail: deposit@ccdc.cam.ac.uk.

Supplementary data associated with this article can be found, in the online version, at doi:10.1016/j.poly.2010.09.027.

References

[1] I. Chopra, J. Antimicrob. Chemother. 59 (2007) 587.
[2] A.D. Russell, W.B. Hugo, Prog. Med. Chem. 31 (1994) 351.
[3] C.F. Shaw III, Chem. Rev. 99 (1999) 2859.
[4] P.J. Barnard, S.J. Berners-Price, Coord. Chem. Rev. 251 (2007) 1889.
[5] H. Tashiro, M. Harigaya, Y. Kageyama, K. Ito, M. Shinotsuka, K. Tani, A. Watada, N. Yiwata, Y. Nakata, S. Emura, Jpn. J. Appl. Phys. 41 (2002) 3758.
[6] M. Péter, T. Schüler, F. Furthner, P.A. Rensing, G.T. van Heck, H.F.M. Schoo, R. Möller, W. Fritzsche, A.J.J.M. Van Breemen, E.R. Meinders, Langmuir 25 (2009) 5384.
[7] M.C. Gimeno, A. Laguna, Comprehensive Coordination Chemistry II, vol. 1, Elsevier, Oxford, 2004.
[8] E. Barreiro, J.S. Casas, M.D. Couce, A. Sánchez, J. Sordo, J.M. Varela, E.M. Vázquez-López, Dalton Trans. (2005) 1707.
[9] E. Barreiro, J.S. Casas, M.D. Couce, A. Sánchez, J. Sordo, J.M. Varela, E.M. Vázquez-López, Z. Anorg. Allg. Chem. 633 (2007) 795.
[10] E. Barreiro, J.S. Casas, M.D. Couce, A. Sánchez, J. Sordo, J.M. Varela, E.M. Vázquez-López, Dalton Trans. (2003) 4754.
[11] E. Barreiro, J.S. Casas, M.D. Couce, A. Sánchez, J. Sordo, J.M. Varela, E.M. Vázquez-López, J. Inorg. Biochem. 102 (2008) 184.
[12] P.D. Cookson, E.R.T. Tiekink, J. Coord. Chem. 26 (1992) 313.
[13] D.R. Smyth, B.R. Vincent, E.R.T. Tiekink, Cryst. Growth Des. 1 (2001) 113.
[14] T.R. Shattock, K.K. Arora, P. Vishweshwar, M.J. Zaworotko, Cryst. Growth Des. 8 (2008) 4533.
[15] C. Gränacher, Helv. Chim. Acta 5 (1922) 610.
[16] E. Campaigne, R.E. Cline, J. Org. Chem. 21 (1956) 32.
[17] F.C. Brown, K. Bradsher, S.G. McCallum, M. Potter, J. Org. Chem. 15 (1950) 174.
[18] P. Álvarez-Boo, J.S. Casas, M.D. Couce, V. Fernández-Moreira, E. Freijanes, E. García-Martínez, J. Sordo, E.M. Vázquez-López, Eur. J. Inorg. Chem. (2005) 4425.
[19] R.A. Stein, C. Knobler, Inorg. Chem. 16 (1977) 242.
[20] SMART and SAINT, Bruker XS Inc., Madison, Wisconsin, USA, 1997.
[21] G.M. Sheldrick, SADABS, University of Göttingen, Germany, 2002.
[22] G.M. Sheldrick, SHELX-97, Program for the Solution and Refinement of Crystal Structures, University of Göttingen, Germany, 1997.
[23] I.J. Bruno, J.C. Cole, P.R. Edgington, M.K. Kessler, C.F. Macrae, P. McCabe, J. Pearson, R. Taylor, Acta Crystallogr., Sect. B 58 (2002) 389.
[24] K. Nomiya, R. Noguchi, T. Shigeta, Y. Kondoh, K. Tsuda, K. Ohsawa, N. Chikaraishi-Kasuga, M. Oda, Bull. Chem. Soc. Jpn. 73 (2000) 1143.
[25] K. Nomiya, N.C. Kasuga, I. Takamori, K. Tsuda, Polyhedron 17 (1998) 3519.
[26] G.E. Maciel, R.V. James, Inorg. Chem. 11 (1964) 1650.
[27] S. Zeltner, S. Jelonek, J. Sielen, R.M. Olk, Eur. J. Inorg. Chem. (2001) 1535.
[28] G. Buemi, F. Zuccarello, J. Mol. Struct. (Teochem) 581 (2002) 71.
[29] L. Norskov-Lauritsen, L. Carlsen, F. Duus, J. Chem. Soc., Chem. Commun. (1983) 496.
[30] T. Steiner, Chem. Commun. (1998) 411.
[31] P.E. Bourne, M.R. Taylor, Acta Crystallogr., Sect. C39 (1983) 266.
[32] E. Barreiro, J.S. Casas, M.D. Couce, A. Gato, A. Sánchez, J. Sordo, J.M. Varela, E.M. Vázquez-López, Inorg. Chem. 47 (2008) 6262.
[33] E. Barreiro, J.S. Casas, M.D. Couce, A. Sánchez, J. Sordo, J.M. Varela, E.M. Vázquez-López, Cryst. Growth Des. 7 (2007) 1964.